

Supplementary Materials

Self-Assembling Lectin Nano-Block Oligomers Enhance Binding Avidity to Glycans

**Shin Irumagawa^{1,2,3}, Keiko Hiemori⁴, Sayoko Saito⁴, Hiroaki Tateno⁴
and Ryoichi Arai^{1,2,3,*}**

¹ Department of Biomolecular Innovation, Institute for Biomedical Sciences,
Interdisciplinary Cluster for Cutting Edge Research, Shinshu University, Ueda, Nagano
386-8567, Japan

² Department of Applied Biology, Faculty of Textile Science and Technology, Shinshu
University, Ueda, Nagano 386-8567, Japan

³ Department of Science and Technology, Graduate School of Medicine, Science and
Technology, Shinshu University, Ueda, Nagano 386-8567, Japan

⁴ Cellular and Molecular Biotechnology Research Institute, National Institute of
Advanced Industrial Science and Technology (AIST), Tsukuba, Ibaraki 305-8566, Japan

* Correspondence: rarai@shinshu-u.ac.jp

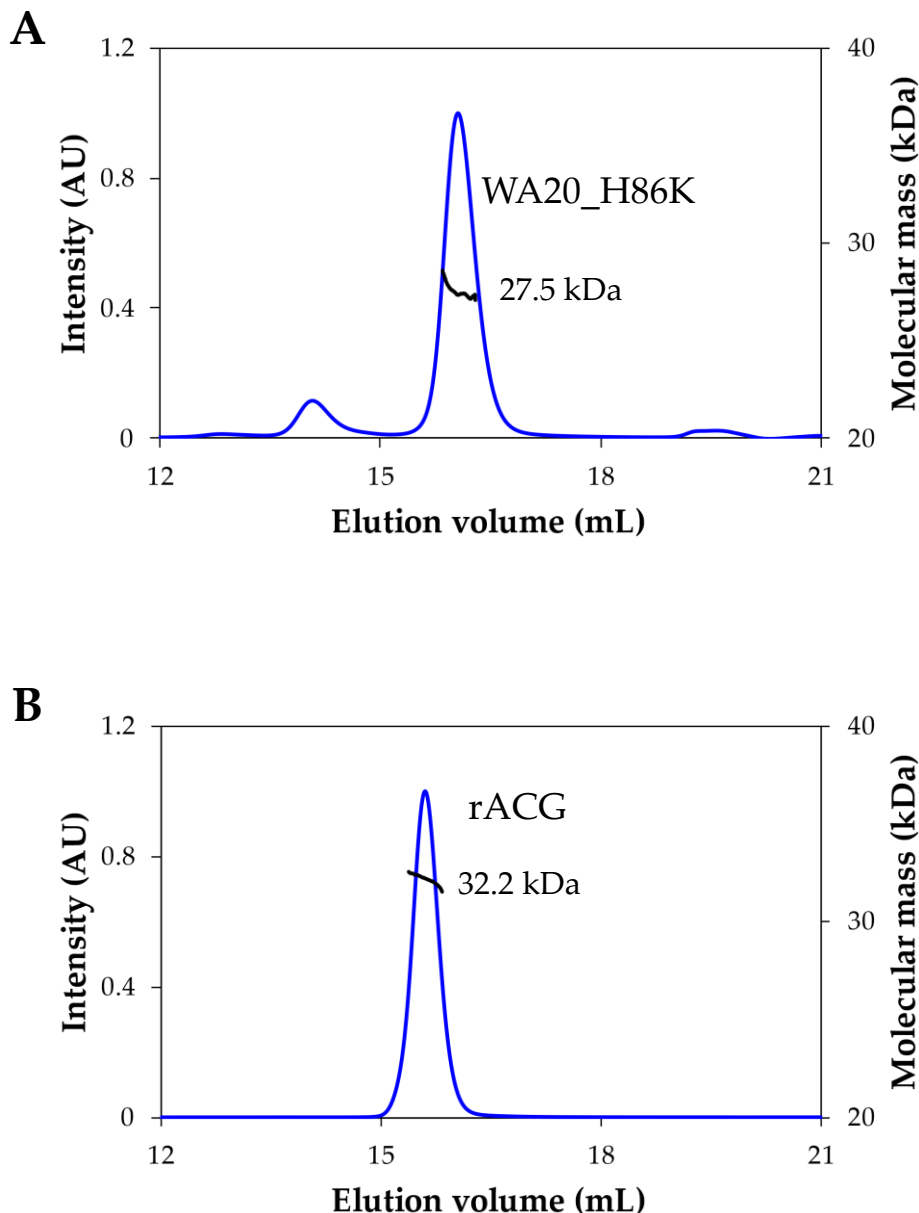


Figure S1. Size exclusion chromatography–multi angle light scattering (SEC–MALS) profiles of (A) de novo protein WA20_H86K mutant and (B) recombinant *Agrocybe cylindracea* galectin (rACG).

The blue and black lines represent the normalized intensity of UV absorbance ($A_{280\text{nm}}$) and the molecular mass of the protein, respectively. The molecular mass values of WA20_H86K and rACG were calculated to be 27.5 kDa and 32.2 kDa, respectively. Because the theoretical molecular mass values of a WA20_H86K monomer and a rACG monomer are 12.5 kDa and 17.0 kDa, respectively, Both proteins formed dimers in solution.

WA20-HL4-ACG (*m*: 32.1 kDa)

MYGKLNLKVE HIKELLQQQLN KNWHRHQGNL HDMNQQMEQL FQEFOHFMQG
NQDDGKLQNM IHEMQQFMNQ VDNHLQSESD TVHHFKNKLQ ELMNNFHHLV
HRKLAEAAAK EAAAKEAAAK EAAAAKAAAHM TTSAVNIYNI SAGASVDLAA
PVTTGDIVTF FSSALNLSAG AGSPNNNTALN LLSENGAYLL HIAFRLQENV
IVFNSRQPNA PWLVEQRVSN VANQFIGSGG KAMVTVFDHG DKYQVVINEK
TVIQYTKQIS GTTSSLSSYNS TEGTSIFSTV VEAVTYTGLA

WA20-FL4-ACG (*m*: 31.5 kDa)

MYGKLNLKVE HIKELLQQQLN KNWHRHQGNL HDMNQQMEQL FQEFOHFMQG
NQDDGKLQNM IHEMQQFMNQ VDNHLQSESD TVHHFKNKLQ ELMNNFHHLV
HRKLSGGGGS GGGGSGGGGS GGGGSAAAHM TTSAVNIYNI SAGASVDLAA
PVTTGDIVTF FSSALNLSAG AGSPNNNTALN LLSENGAYLL HIAFRLQENV
IVFNSRQPNA PWLVEQRVSN VANQFIGSGG KAMVTVFDHGDKYQVVINEK
TVIQYTKQIS GTTSSLSSYNS TEGTSIFSTV VEAVTYTGLA

WA20-SL-ACG (*m*: 30.1 kDa)

MYGKLNLKVE HIKELLQQQLN KNWHRHQGNL HDMNQQMEQL FQEFOHFMQG
NQDDGKLQNM IHEMQQFMNQ VDNHLQSESD TVHHFKNKLQ ELMNNFHHLV
HRKLAAAHMT TSAVNIYNIS AGASVDLAAP VTTGDIVTF SSALNLSAGA
GSPNNNTALNL LSENGAYLL IAFRLQENVI VFNSRQPNA WLVEQRVSNV
ANQFIGSGGK AMVTVFDHGD KYQVVINEKT VIQYTKQISG TTSSLSSYNST
EGTSIFSTVV EAVTYTGLA

WA20-H-ACG (*m*: 29.7 kDa)

MYGKLNLKVE HIKELLQQQLN KNWHRHQGNL HDMNQQMEQL FQEFOHFMQG
NQDDGKLQNM IHEMQQFMNQ VDNHLQSESD TVHHFKNKLQ ELMNNFHHLV
HRHMTTSAVN IWNISAGASV DLAAPVTTGD IVTFFSSALN LSAGAGSPNN
TALNLLSENG AYLLHIAFRL QENVIVFNSR QPNAPWLVEQ RVSNVANQFI
GSGGKAMVTV FDHGDKYQVV INEKTVIQT KQISGTSSL SYNSTEGTSI
FSTVVEAVTY TGLA

WA20-ΔN3ACG (*m*: 29.2 kDa)

MYGKLNLKVE HIKELLQQQLN KNWHRHQGNL HDMNQQMEQL FQEFOHFMQG
NQDDGKLQNM IHEMQQFMNQ VDNHLQSESD TVHHFKNKLQ ELMNNFHHLV
HRSAVNIYNI SAGASVDLAA PVTTGDIVTF FSSALNLSAG AGSPNNNTALN
LLSENGAYLL HIAFRLQENV IVFNSRQPNA PWLVEQRVSN VANQFIGSGG
KAMVTVFDHG DKYQVVINEK TVIQYTKQIS GTTSSLSSYNS TEGTSIFSTV
VEAVTYTGLA

Figure S2. Amino acid sequences of lectin nano-blocks.

Blue, red, and black letters represent the sequences of WA20_H86K, ACG, and peptide linker, respectively. The *m* means the theoretical molecular mass of a monomer of each lectin nano-block.

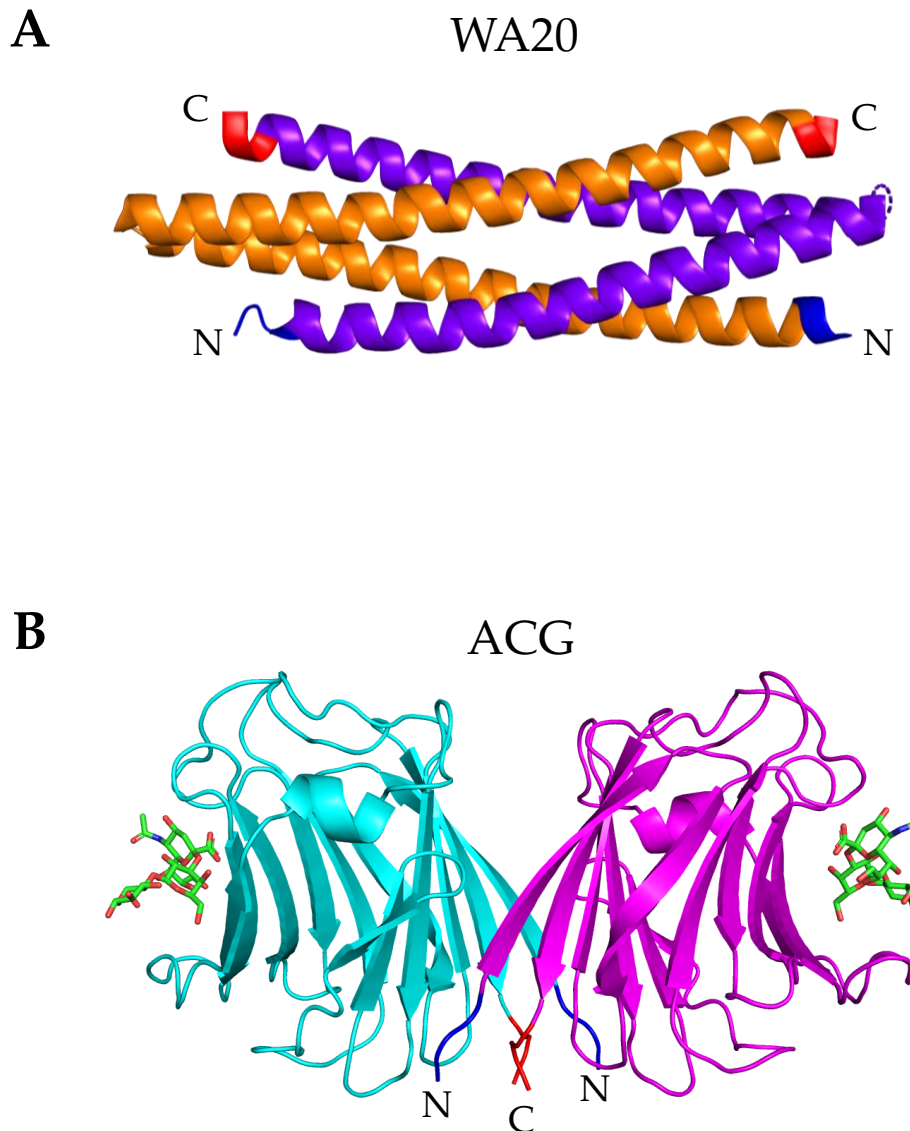
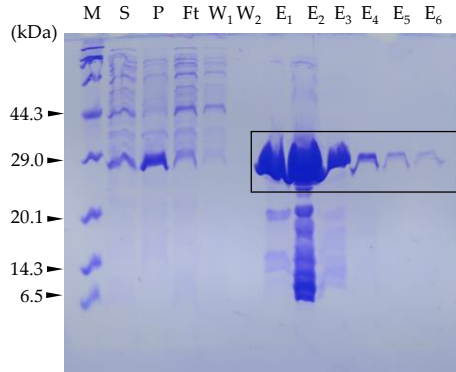


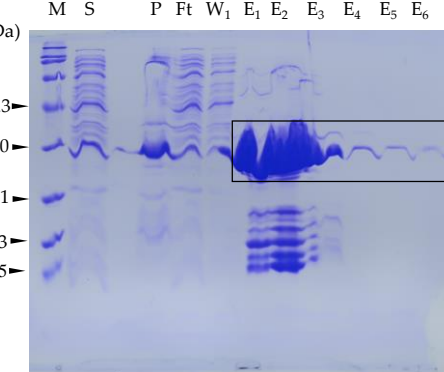
Figure S3. Crystal structures of WA20 and ACG.

The dimer structures of (A) WA20 (PDB ID: 3VJF) [9] and (B) ACG (PDB ID: 1WW4) [30]. (A) Chains A and B of WA20 are shown in orange and purple, respectively. The residues of N-termini (chain A: 3–5, chain B: 5–7) and C-termini (chain A and B: 99–101) are shown in blue and red, respectively. (B) Chains A and D of ACG are shown in magenta and cyan, respectively. Two NeuAc α 2-3lactose shown as sticks. The residues of N-termini (chain A and D: 2–4) and C-termini (chain A and D: 159–161) residues are shown in blue and red, respectively.

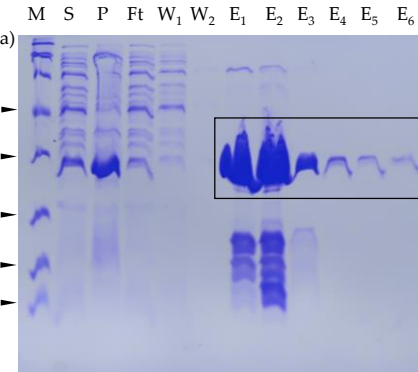
WA20-HL4-ACG



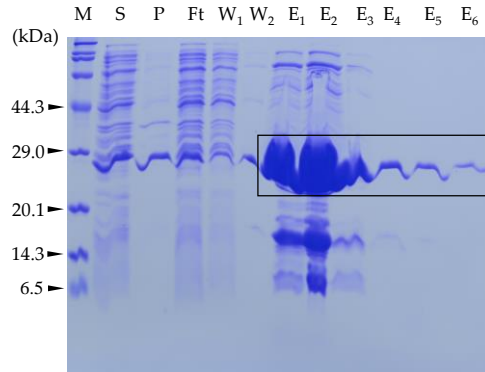
WA20-FL4-ACG



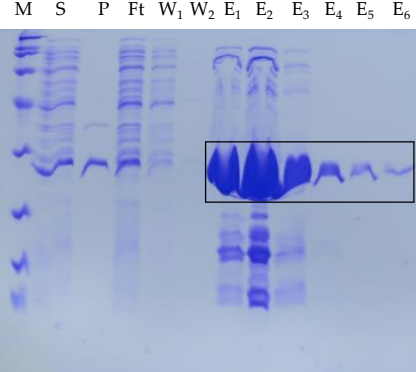
WA20-SL-ACG



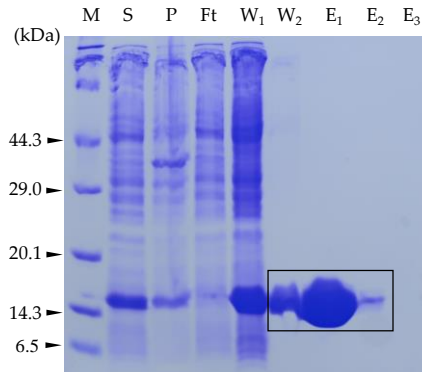
WA20-H-ACG



WA20-ΔN3ACG



rACG



WA20

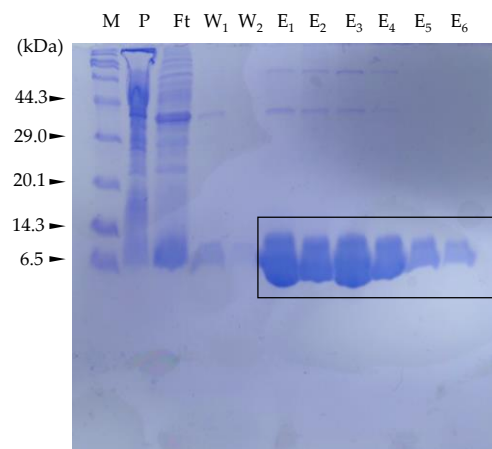
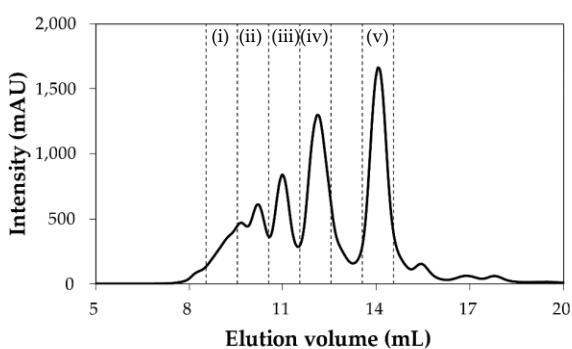
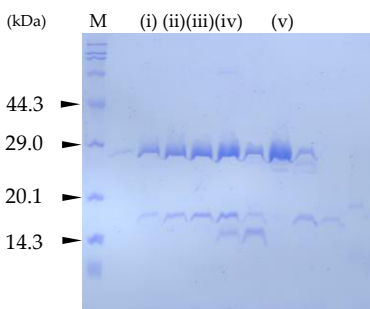
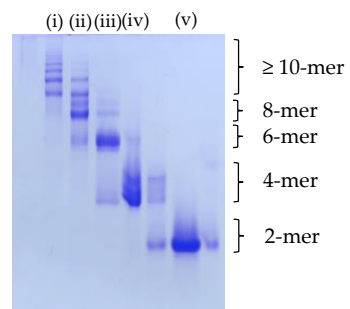


Figure S4. Sodium dodecyl sulfate polyacrylamide gel electrophoresis (SDS-PAGE) analysis. SDS-PAGE analysis of the five lectin nano-blocks and WA20 were performed for the eluted fractions by immobilized metal ion affinity chromatography (IMAC) with TALON metal affinity resin (Takara Bio, Kusatsu, Shiga, Japan), and recombinant ACG (rACG) was performed for the eluted fractions by lactose-immobilized Sepharose column. The protein bands in black rectangles show purified proteins. Protein molecular weight markers (broad) (Takara Bio) are shown in the far-left lane. Proteins were stained with Coomassie brilliant blue. Abbreviations: M, molecular weight marker; S, supernatant fraction; P, pellet fraction; Ft, flow-through fraction; W, wash fractions; E, eluted fractions.

A

WA20-SL-ACG

**B****C**

WA20-H-ACG

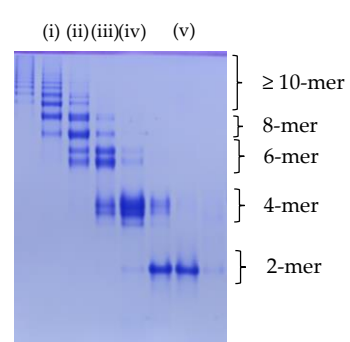
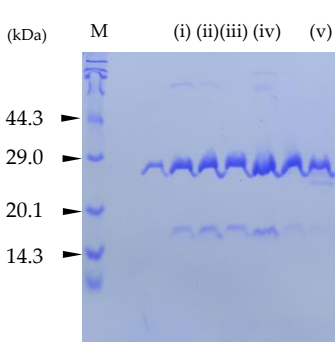
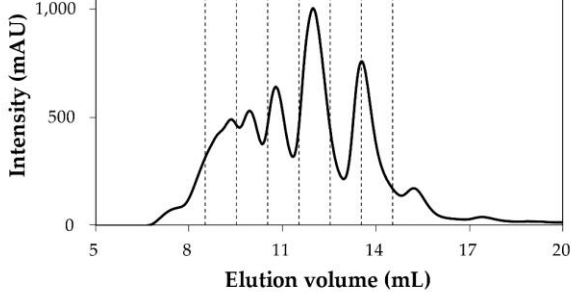
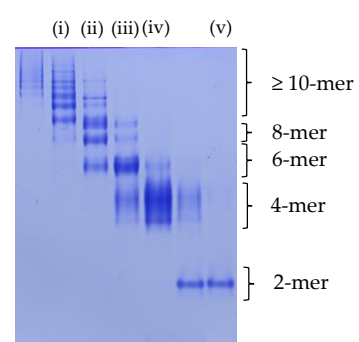
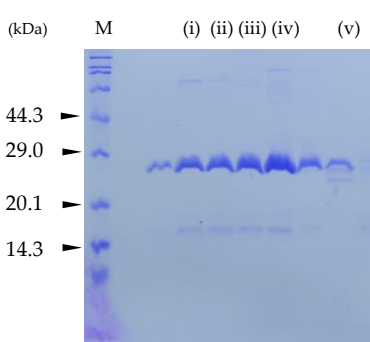
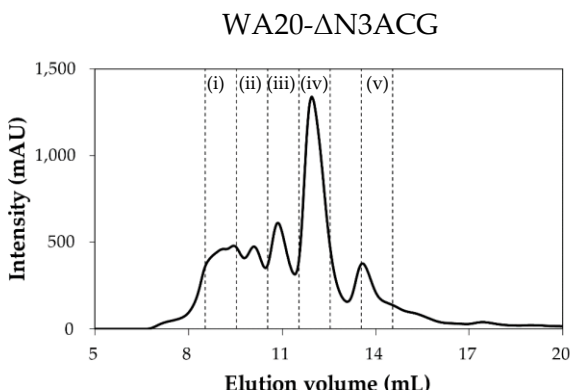
WA20- Δ N3ACG

Figure S5. Size exclusion chromatography (SEC) purification of lectin nano-blocks for small-angle X-ray scattering (SAXS) experiments.

(A) SEC purification profiles of the IMAC-purified samples of WA20-SL-ACG (upper panel), WA20-H-ACG (middle panel), and WA20- Δ N3ACG (lower panel) with a Superdex 200 increase 10/300 GL column (Cytiva). The eluted fractions, Fr. (i), (ii), (iii), (iv), and (v) were used as samples for SAXS experiments of the lectin nano-block oligomers.

(B) SDS-PAGE and (C) native PAGE were performed for the fractionated samples. Proteins were stained with Coomassie brilliant blue. The oligomeric states of the protein bands in native PAGE were estimated from the SEC-MALS results.

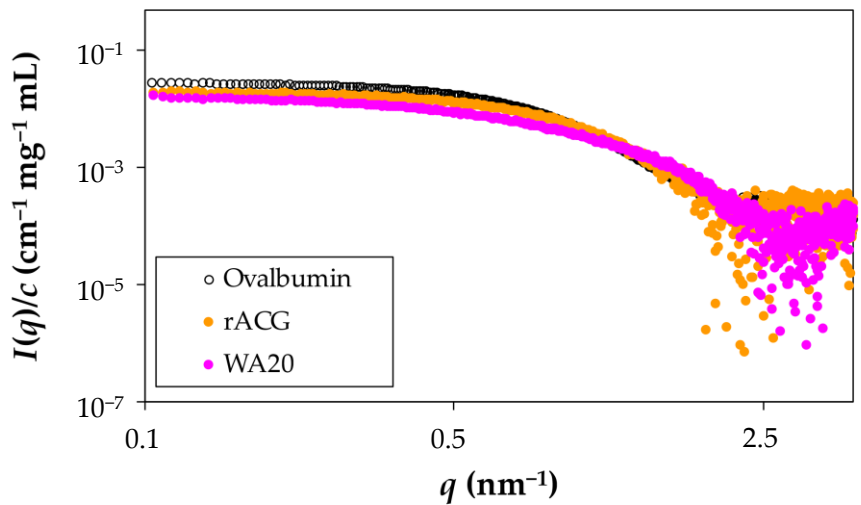
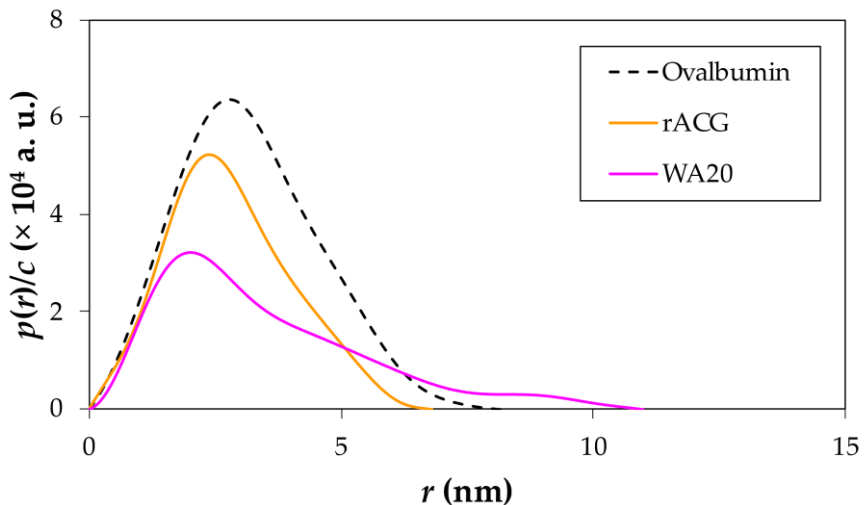
A**B**

Figure S6. SAXS analysis of WA20, rACG, and ovalbumin.

(A) Concentration-normalized absolute scattering intensities of ovalbumin, WA20, and rACG. Ovalbumin was used as a reference standard of the molecular mass.
(B) Pair-distance distribution functions normalized by the concentration, $p(r)/c$, are obtained by inverse Fourier transformation.

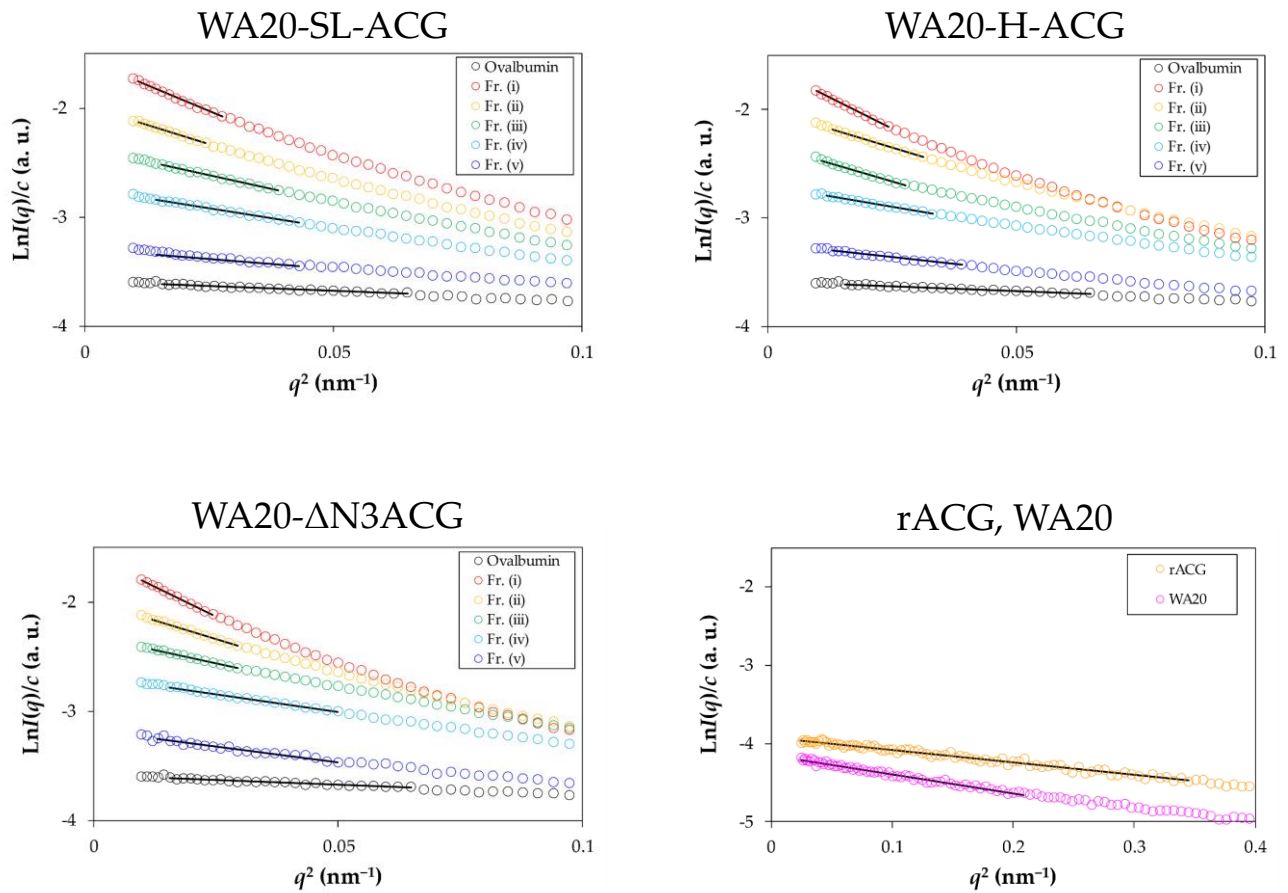


Figure S7. Guinier plots of the lectin nano-blocks, rACG, and WA20.

Forward scattering intensity $I(q \rightarrow 0)$ and radius of gyration R_g of the lectin nano-block oligomers were estimated based on their SAXS data by Guinier approximation using the AUTORG program in ATSAS [50] with SAngler [48].

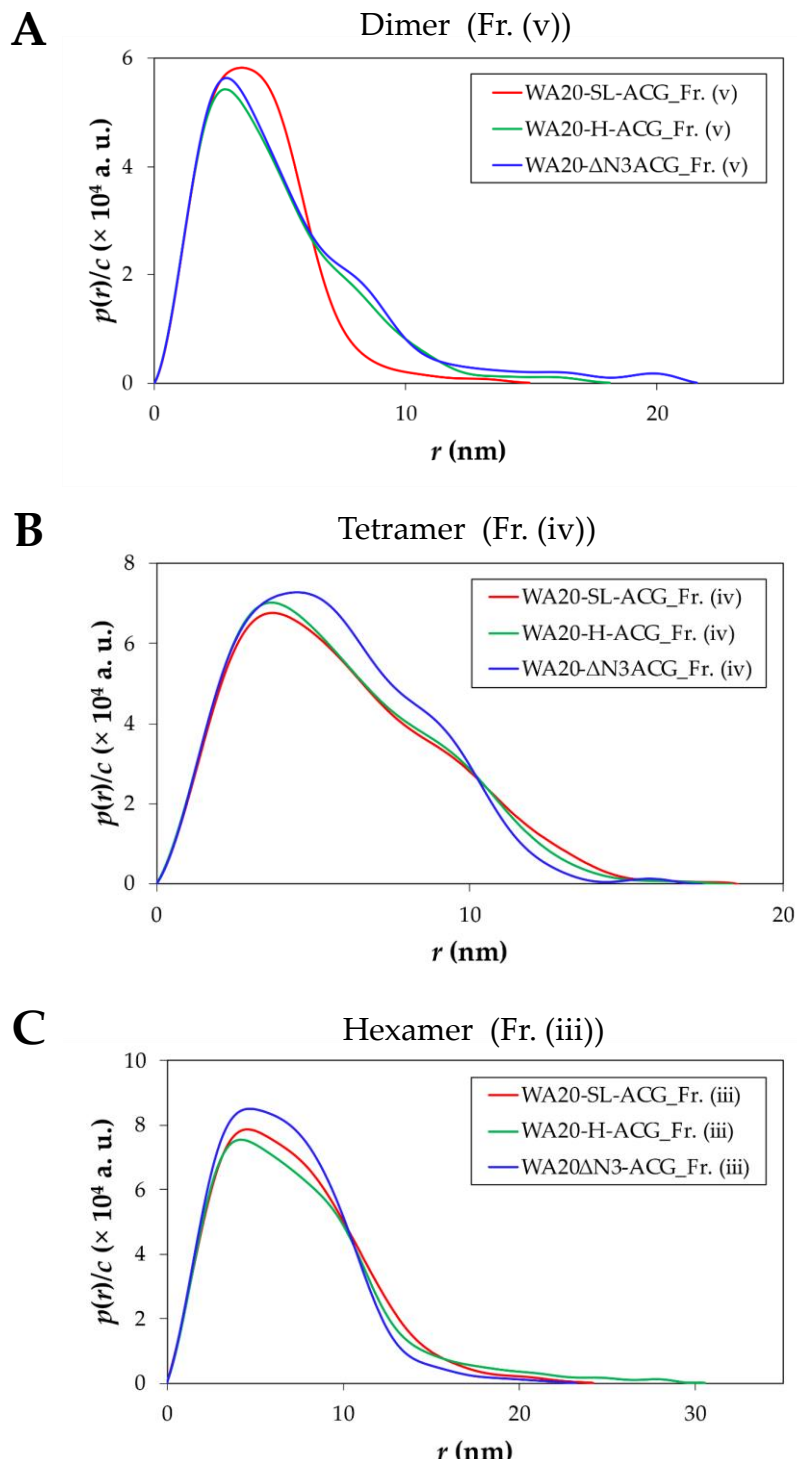


Figure S8. Comparisons of the $p(r)$ functions for (A) dimer, (B) tetramer, and (C) hexamer of the lectin nano-blocks.

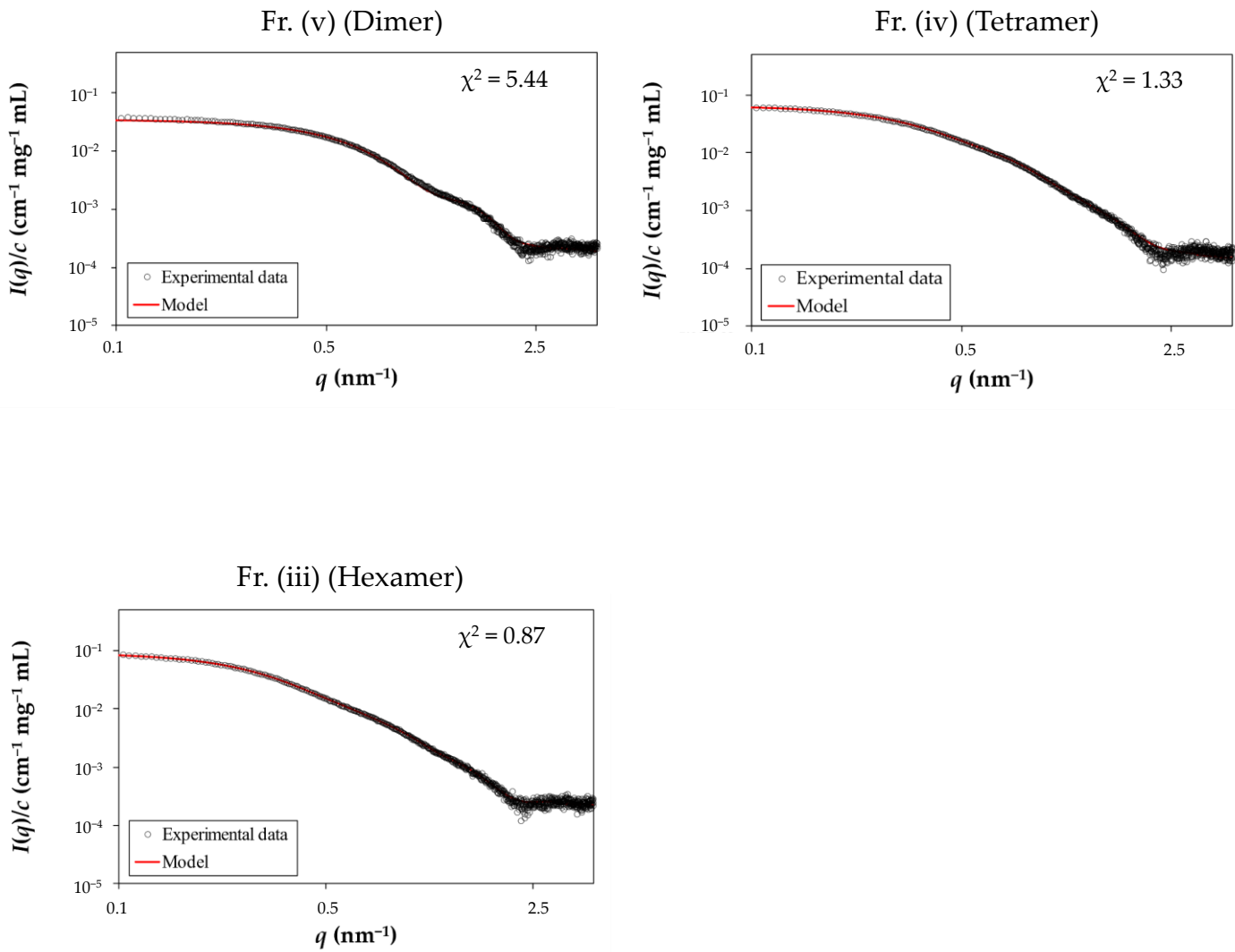


Figure S9. Plots of the scattering curves calculated from the CORAL models of WA20-SL-ACG oligomers fitting to the experimental SAXS data.

The concentration-normalized SAXS intensity $I(q)/c$ of the fractionated samples (Fr.) of WA20-SL-ACG (black open circle) and that optimized by the CORAL procedure (red line). The χ^2 value represents the degree of fitting between the experimental data and the data calculated from the CORAL model.

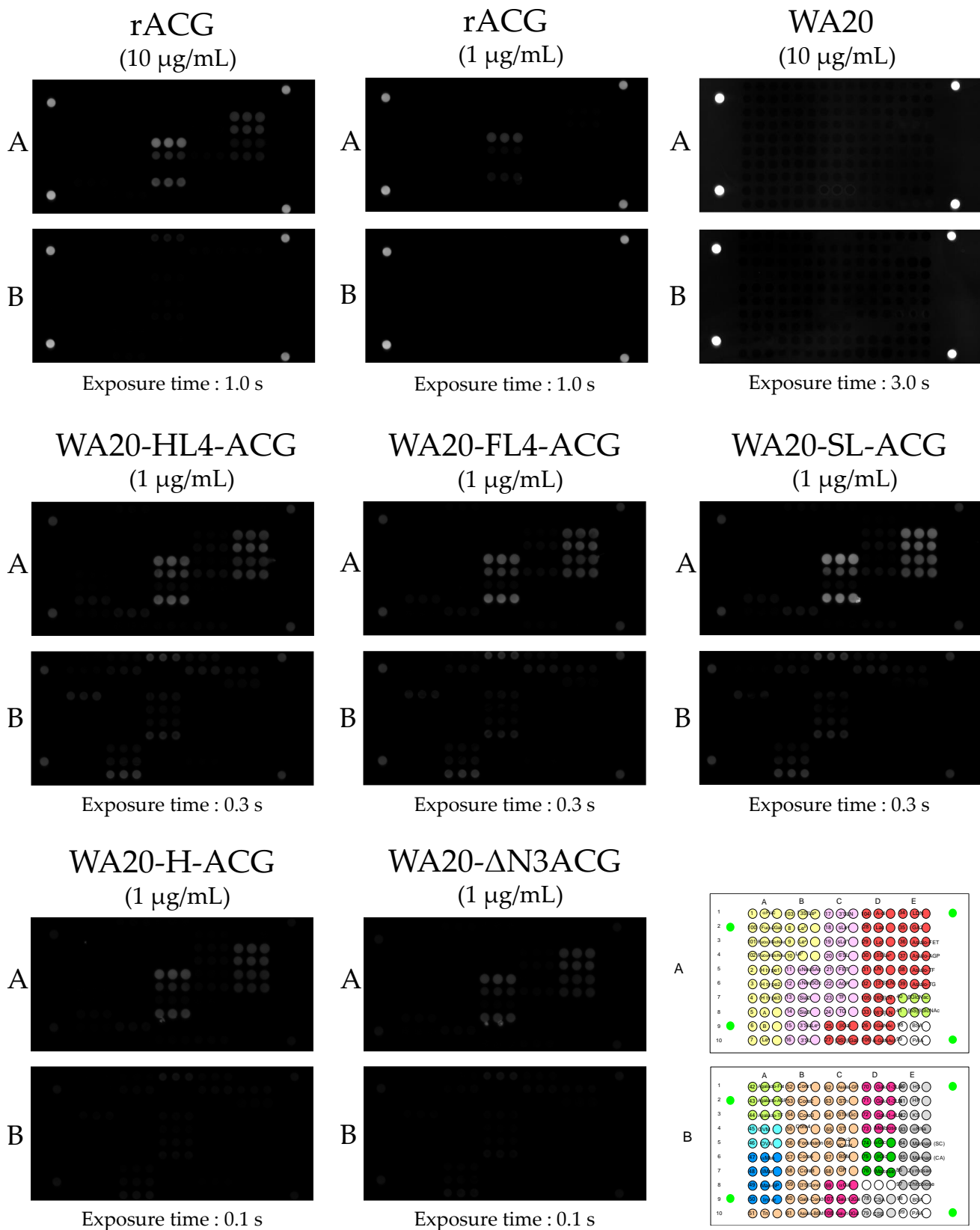


Figure S10. Fluorescence images of glycoconjugate microarray experiments.
The list of glycans used for glycoconjugate microarray analysis is shown in Table S1.

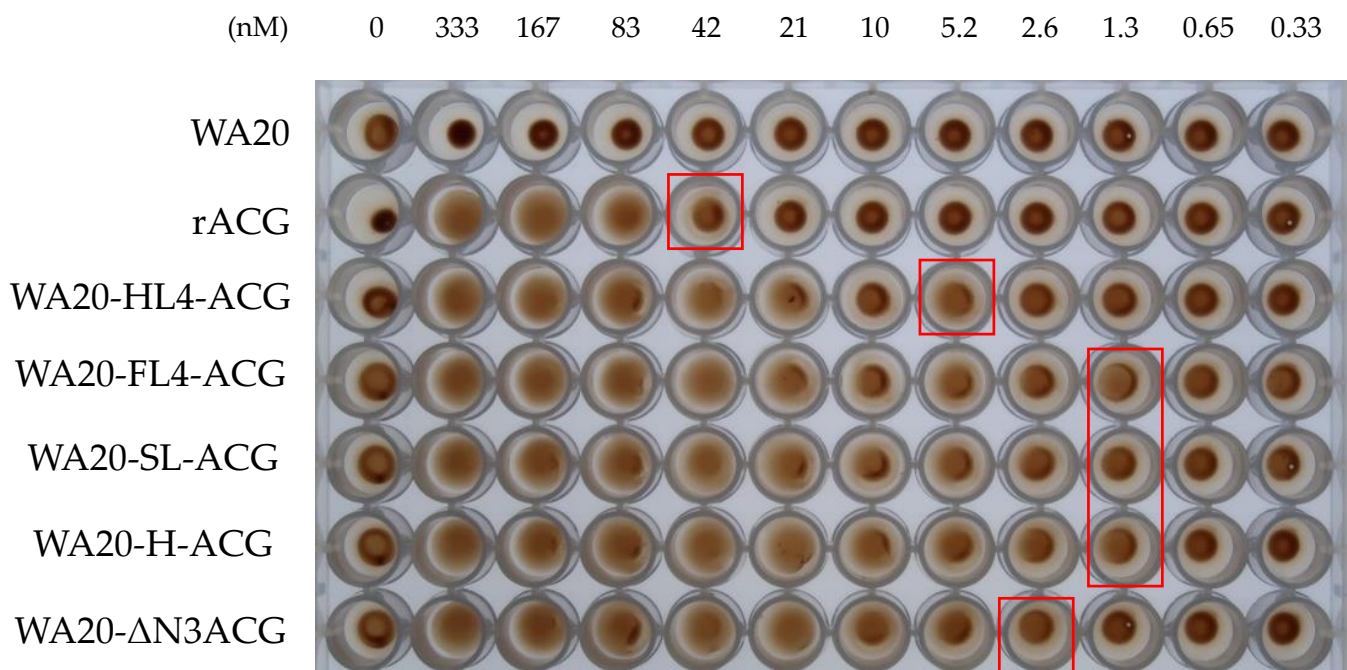


Figure S11. Hemagglutination assay results.

Hemagglutination assay was performed for WA20, rACG, and the five lectin nano-blocks. The wells surrounded by red frames show the minimum concentration of the samples with hemagglutination activity.

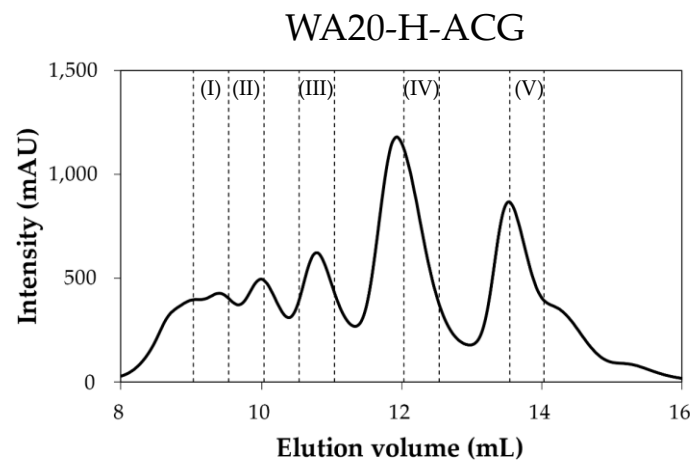
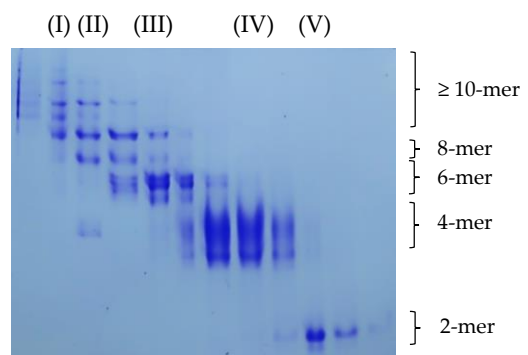
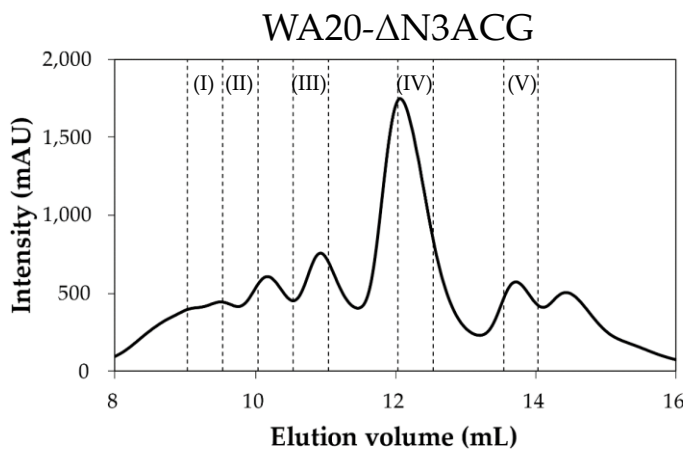
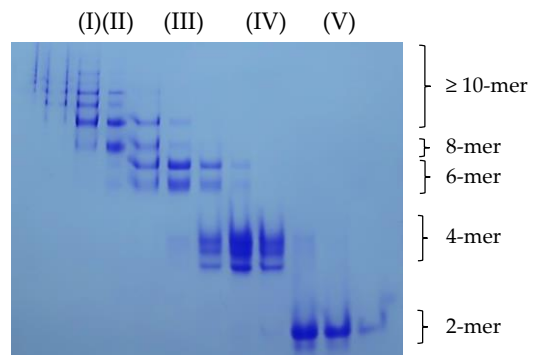
A**B**

Figure S12. SEC purification of lectin nano-blocks for surface plasmon resonance (SPR) experiments.

(A) SEC purification of the IMAC-purified samples of the lectin nano-blocks WA20-H-ACG (upper panel) and WA20- Δ N3ACG (lower panel) with a Superdex 200 increase 10/300 GL column (Cytiva). The eluted fractions (I), (II), (III), (IV), and (V) were used as the samples of the lectin nano-block oligomers for SPR experiments. (B) Native PAGE analysis of the eluted fractions.

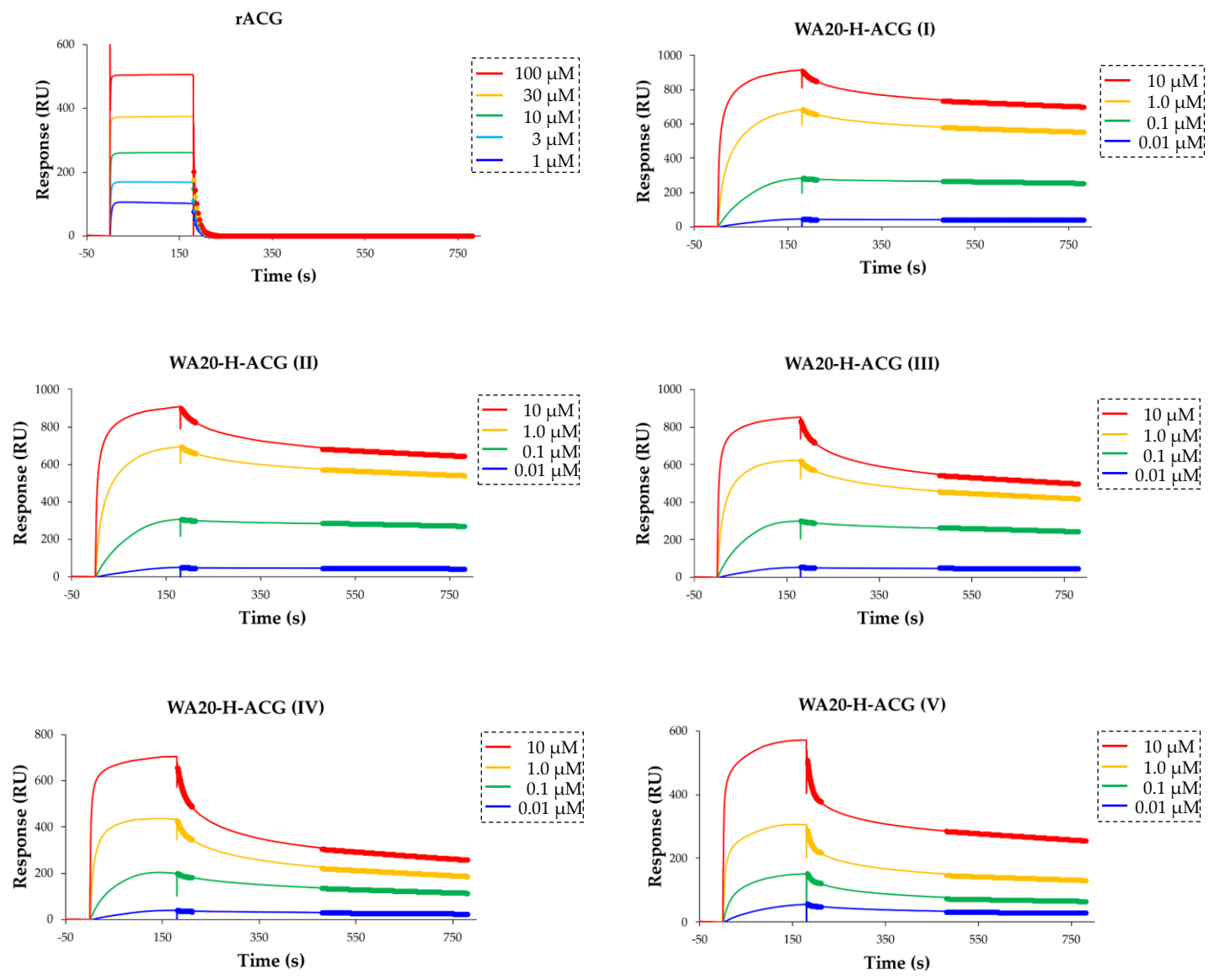


Figure S13. SPR analysis of the WA20-H-ACG oligomers and rACG.

Sensorgrams of the WA20-H-ACG oligomers and rACG at several concentrations, bound to immobilized Neu5Ac α 2-3Gal β 1-4Glc β -Gly-PAA-biotin ligands. Bold lines show the fitting curves used for calculating the apparent dissociation rate constants $k_{d_app_early}$ in the early phase (181–211 s) and $k_{d_app_late}$ in the late phase (480–780 s) of the lectin nano-block oligomers. The apparent dissociation rate constant k_{d_app} of rACG was calculated using the data in the entire dissociation time (181–780 s).

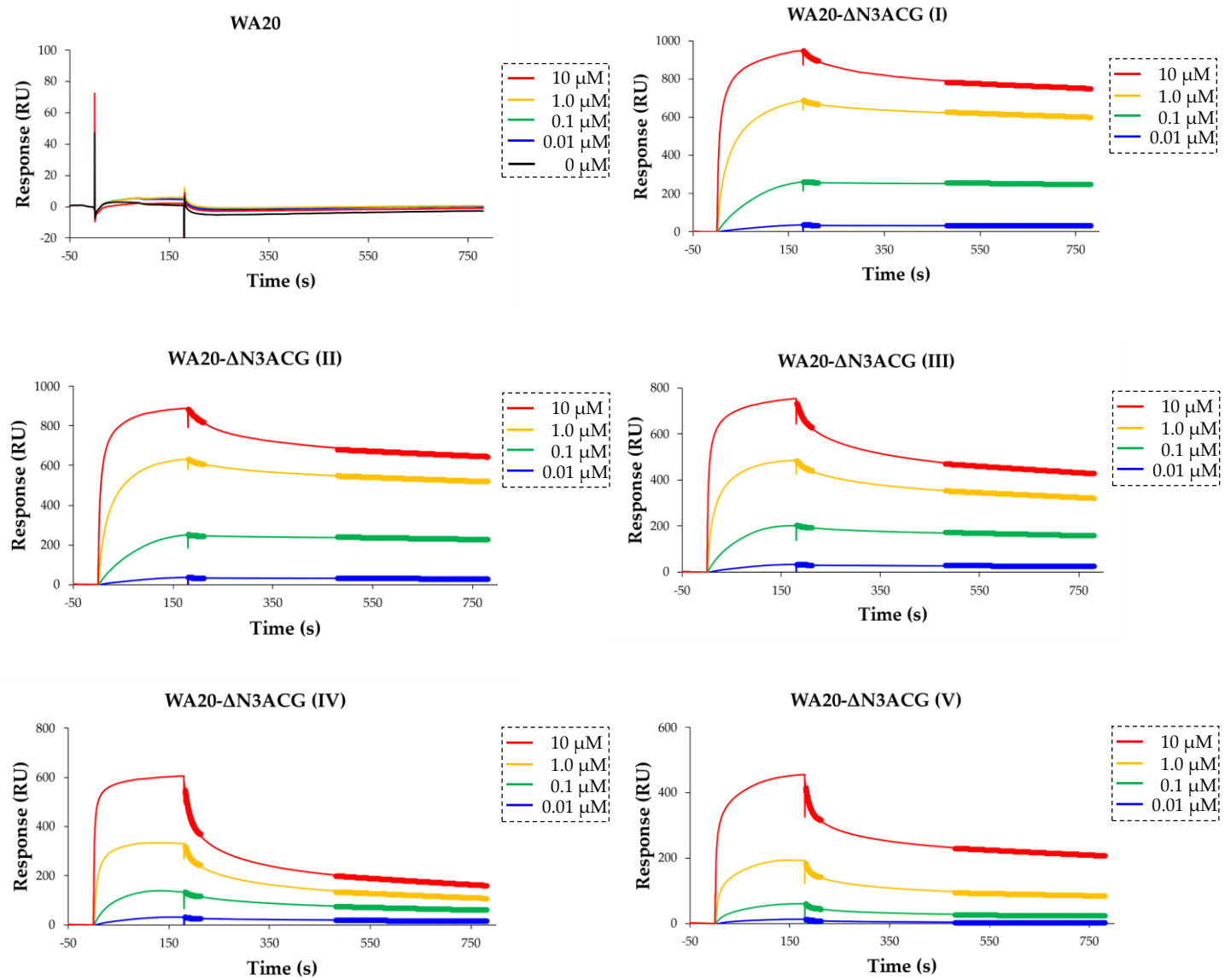
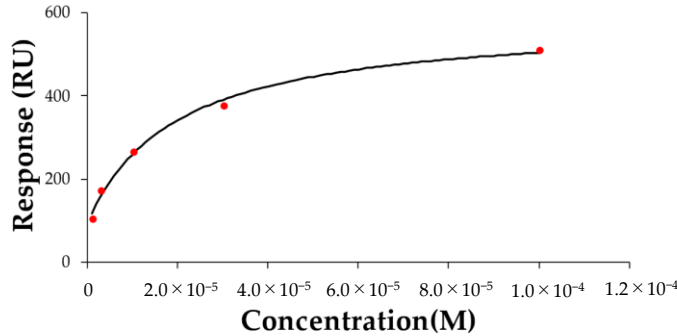
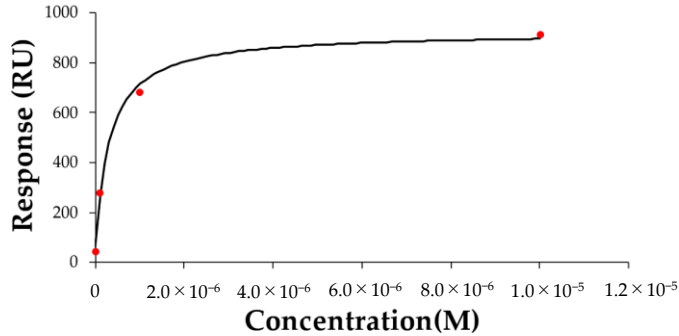


Figure S14. SPR analysis of the WA20- Δ N3ACG oligomers and WA20. Sensorgrams of the WA20- Δ N3ACG oligomers and WA20 at several concentrations, bound to immobilized Neu5Ac α 2-3Gal β 1-4Glc β -Gly-PAA-biotin ligands. Bold lines show the fitting curves used for calculating the apparent dissociation rate constants $k_{d_app_early}$ in the early phase (181–211 s) and $k_{d_app_late}$ in the late phase (480–780 s) of the lectin nano-block oligomers. The apparent dissociation rate constant k_{d_app} of rACG was calculated using the data in the entire dissociation time (181–780 s).

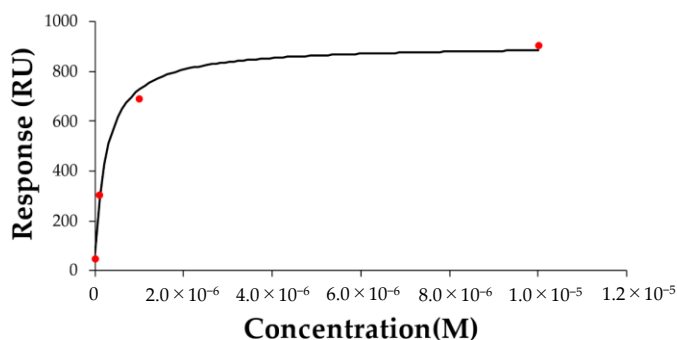
rACG



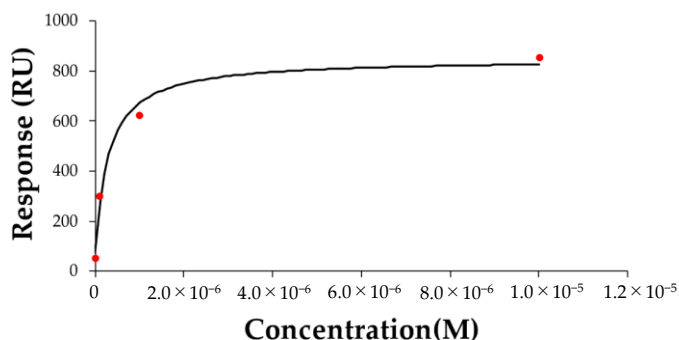
WA20-H-ACG (I)



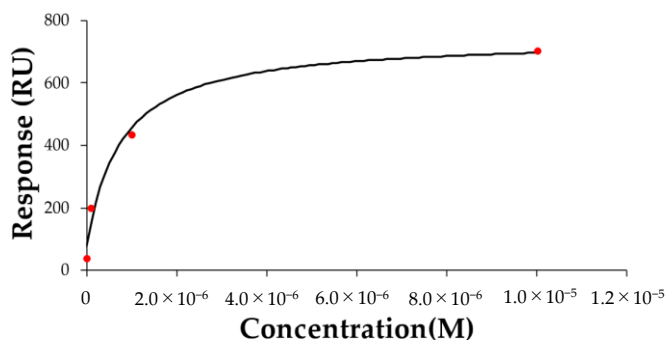
WA20-H-ACG (II)



WA20-H-ACG (III)



WA20-H-ACG (IV)



WA20-H-ACG (V)

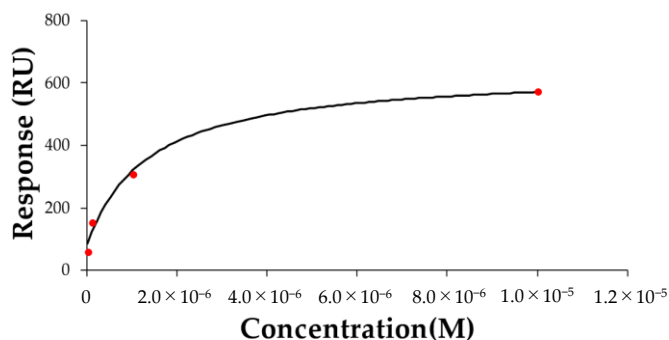


Figure S15. Steady state analysis of SPR data of the WA20-H-ACG oligomers and rACG. The calculation of apparent amount of maximum binding (R_{\max_app}) and apparent dissociation constant (K_{D_app}) was performed by approximately fitting the data at several protein concentrations of each sample to the 1:1 binding steady state affinity model in BIAevaluation software (version 3.0) (Cytiva).

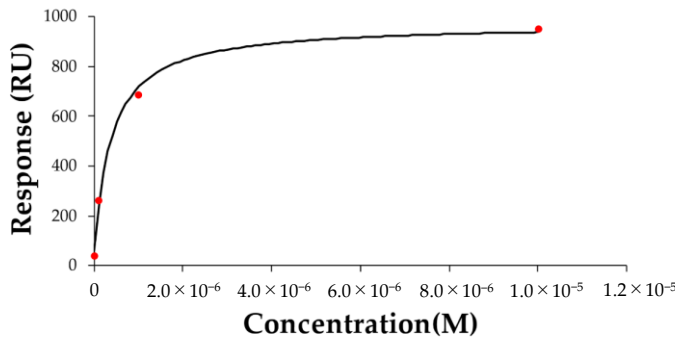
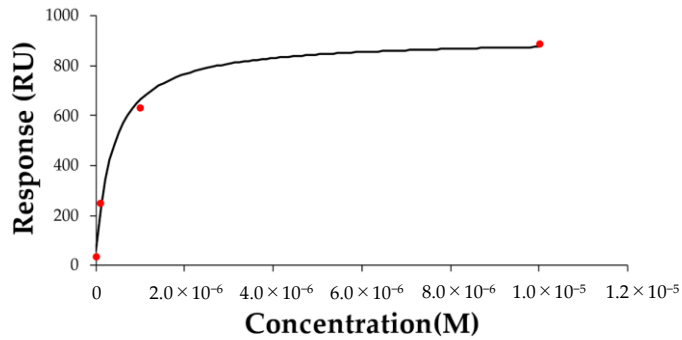
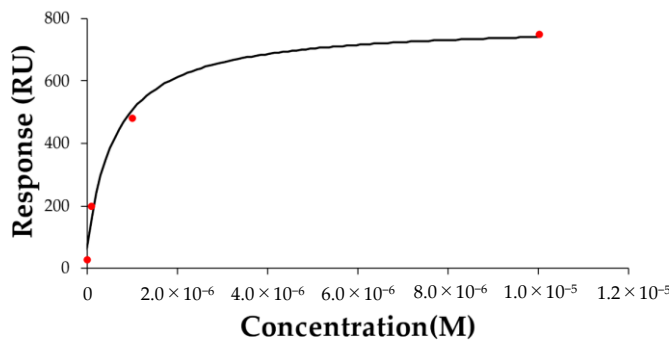
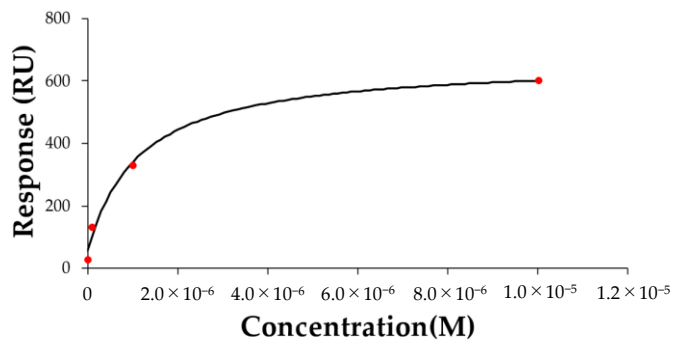
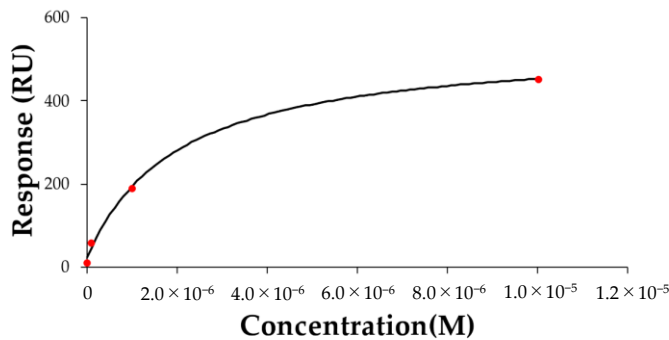
WA20- Δ N3ACG (I)WA20- Δ N3ACG (II)WA20- Δ N3ACG (III)WA20- Δ N3ACG (IV)WA20- Δ N3ACG (V)

Figure S16. Steady state analysis of SPR data of the WA20- Δ N3ACG oligomers. The calculation of the apparent amount of maximum binding (R_{\max_app}) and apparent dissociation constant (K_{D_app}) was performed by approximately fitting the data at several protein concentrations of each sample to the 1:1 binding steady state affinity model in BIAevaluation software (version 3.0) (Cytiva).

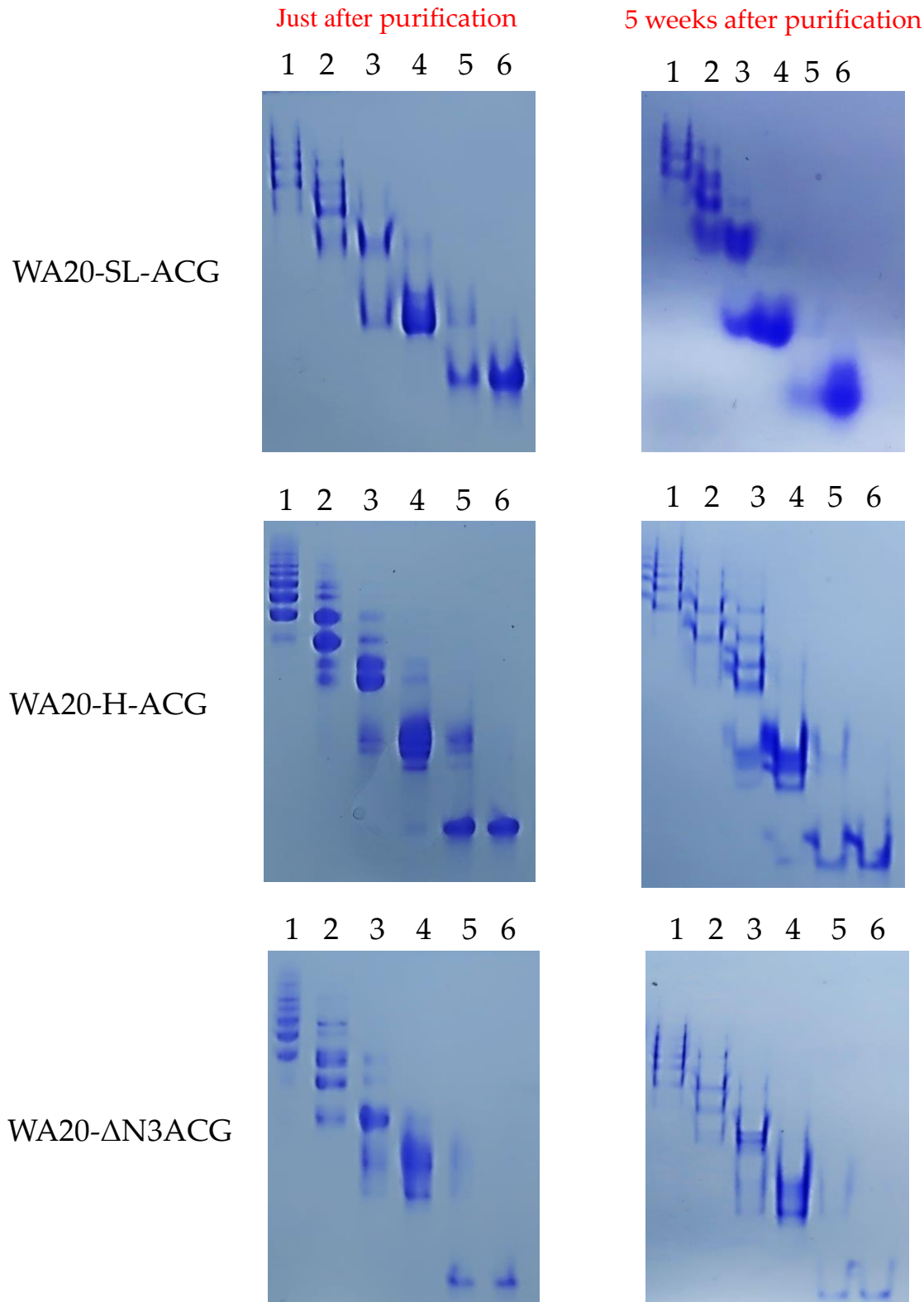


Figure S17. Native PAGE analyses of the lectin nano-block oligomers just after SEC purification and 5 weeks after SEC purification.

Native PAGE of the SEC-fractionated samples of WA20-SL-ACG (top), WA20-H-ACG (middle) and WA20- Δ N3ACG (bottom) with a Superdex 200 increase 10/300 GL column (Cytiva). The fractionated samples were stored at 4 °C for 5 weeks, and then native PAGE of the same samples were performed again.

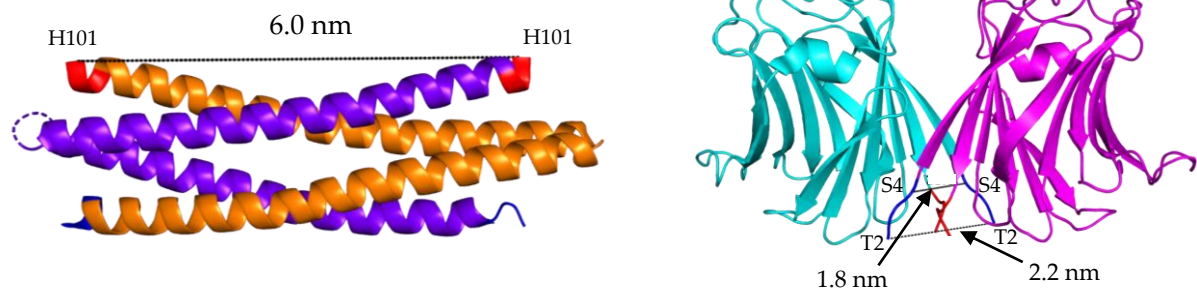
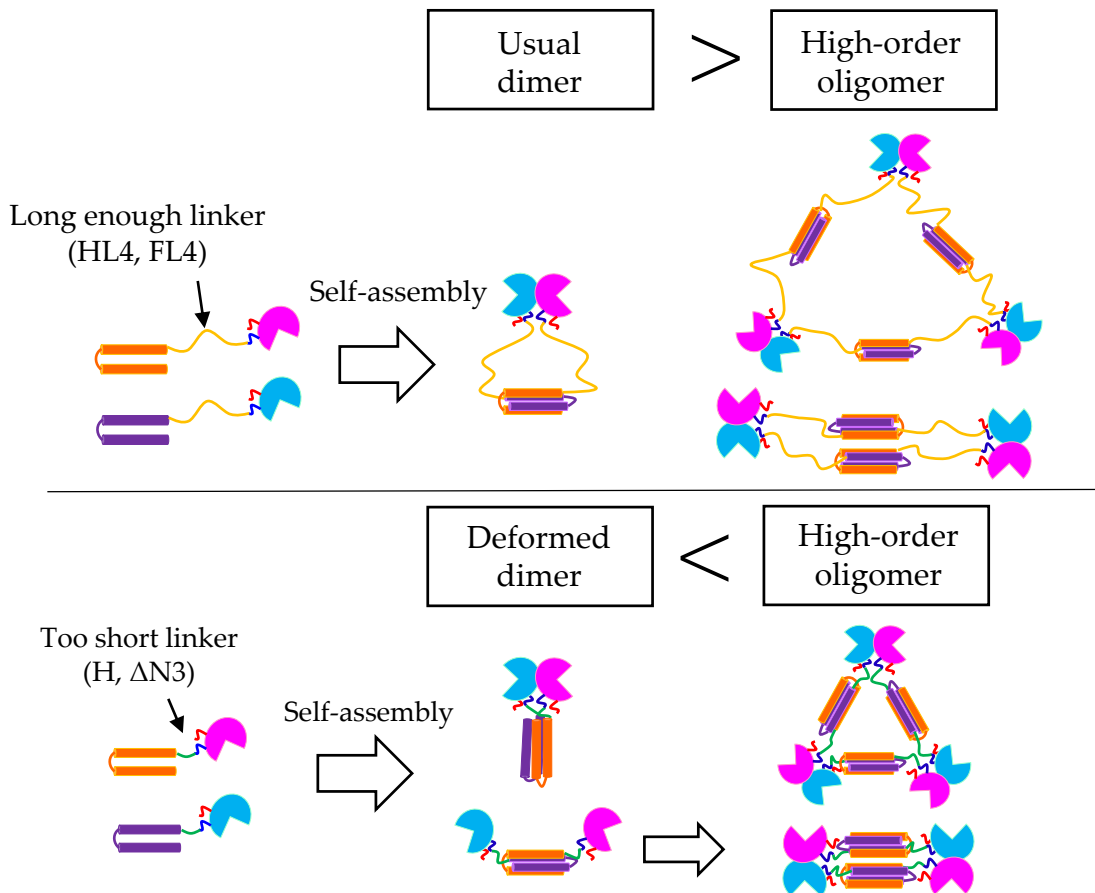
A**B**

Figure S18. Schematic diagrams of oligomerization of the lectin nano-blocks affected by the linker length.

(A) Distance between the C-termini of WA20 (PDB ID: 3VJF) and distance between the N-termini of ACG (PDB ID: 1WW7). (B) Schematic models of oligomerization of the lectin nano-blocks affected by the linker length. When the linker of the lectin nano-blocks between WA20 and ACG is long (FL4, HL4), the lectin nano-blocks preferentially form dimer because of the enough length for both domains of WA20 and ACG to form dimers simultaneously. When the linker of the lectin nano-blocks between WA20 and ACG is too short ($H, \Delta N3$), the lectin nano-blocks preferentially form tetramer and higher oligomers because of the too short linker for both domains of WA20 and ACG to form usual dimers simultaneously.

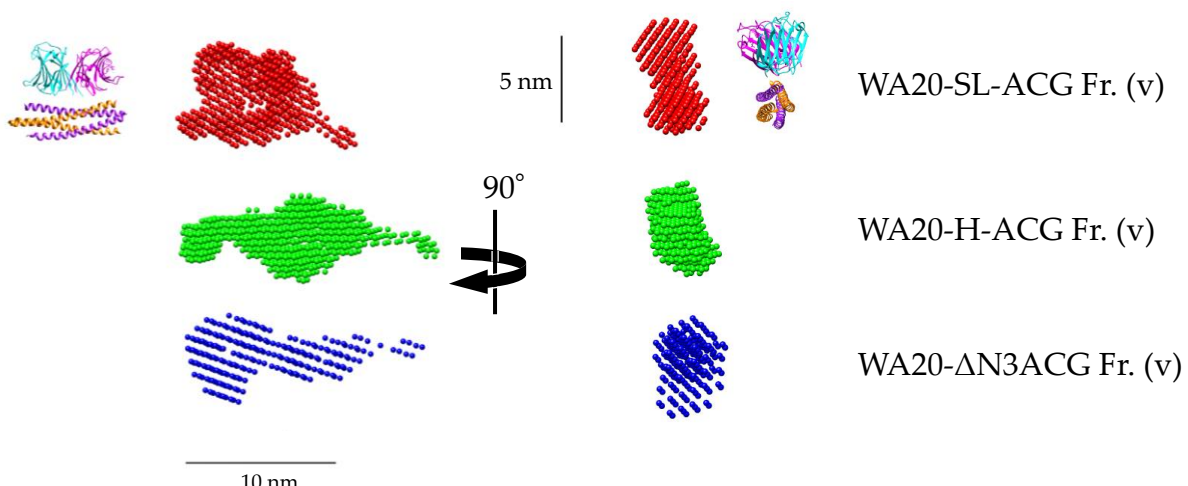
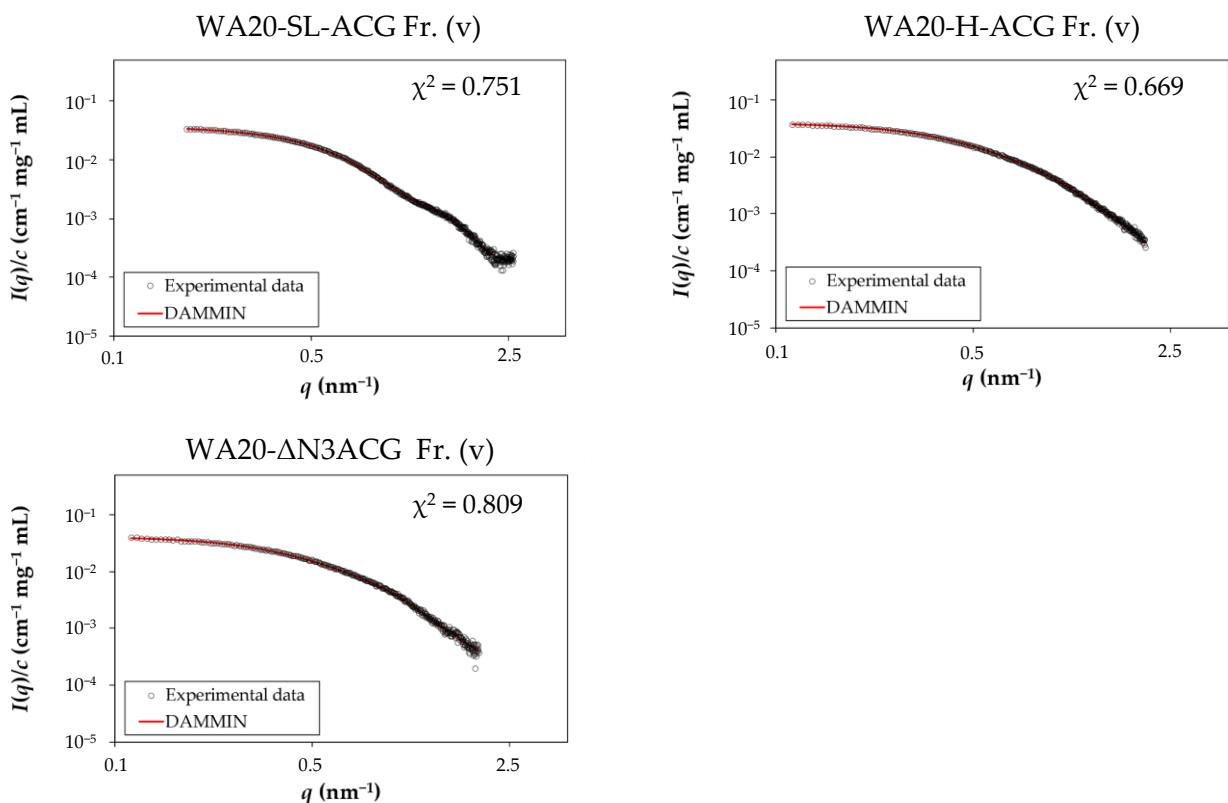
A**B**

Figure S19. Dummy atom modelling of dimers of the lectin nano-blocks.

(A) Dummy atom models of the lectin nano-block dimers of WA20-SL-ACG, WA20-H-ACG, and WA20- Δ N3ACG. The models were constructed based on the SAXS data using the ab initio modelling programs DAMMIF, DAMAVER, and DAMMIN without a symmetry constraint. Ribbon representations of the crystal structures of WA20 (PDB ID: 3VJF) and ACG (PDB ID: 1WW7) are shown as references.

(B) Plots of the scattering curves calculated from the DAMMIN models fitting to the experimental SAXS data. The concentration-normalized SAXS intensity $I(q)/c$ of the lectin nano-block dimers (black open circle) and that optimized by the DAMMIN procedure (red line). The χ^2 value represents the degree of fitting between the experimental data and the data calculated from the DAMMIN model.

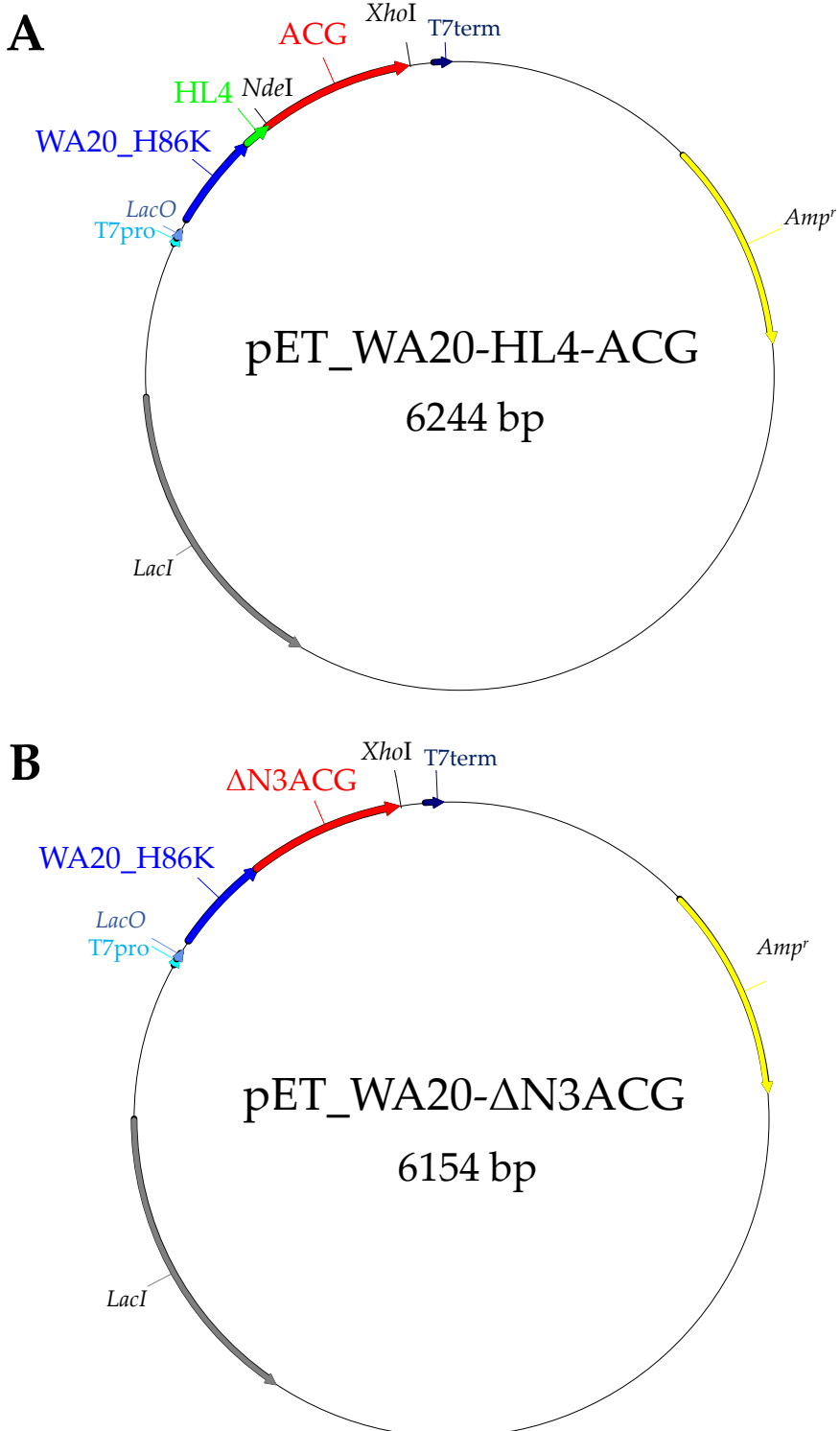


Figure S20. Maps of expression plasmids for the lectin nano-blocks, (A) WA20-HL4-ACG and (B) WA20-ΔN3ACG.

Expression plasmids of the other lectin nano-blocks were constructed by replacing the HL4 linker (green) of pET_WA20-HL4-ACG with the other linker (FL4, SL, or H).

Table S1. The list of glycans used for glycoconjugate microarray analysis.

| Number | Trivial name | Presentation | Glycans |
|--------|--------------------------|--------------|---|
| 1 | α Fuc | PAA | Fuc1-PAA |
| 2 | Fuc α 2Gal | PAA | Fuc α 1-2Gal β 1-PAA |
| 3 | Fuc α 3GlcNAc | PAA | Fuc α 1-3GlcNAc β 1-PAA |
| 4 | Fuc α 4GlcNAc | PAA | Fuc α 1-4GlcNAc β 1-PAA |
| 5 | H type1 | PAA | Fuc α 1-2Gal β 1-3GlcNAc β 1-PAA |
| 6 | H type2 | PAA | Fuc α 1-2Gal β 1-4GlcNAc β 1-PAA |
| 7 | H type3 | PAA | Fuc α 1-2Gal β 1-3GalNAc α 1-PAA |
| 8 | A | PAA | GalNAc α 1-(Fuc α 1-2Gal β 1-4GlcNAc β 1-PAA) |
| 9 | B | PAA | Gal α 1-3(Fuc α 1-2)Gal β 1-4GlcNAc β 1-PAA |
| 10 | Lea | PAA | Gal β 1-3(Fuc α 1-4)GlcNAc β 1-PAA |
| 11 | [3S]Lea | PAA | (3SO ₃)Gal β 1-3(Fuc α 1-4)GlcNAc β 1-PAA |
| 12 | Leb | PAA | Fuc α 1-2Gal β 1-3(Fuc α 1-4)GlcNAc β 1-PAA |
| 13 | Lex | PAA | Gal β 1-4(Fuc α 1-3)GlcNAc β 1-PAA |
| 14 | Ley | PAA | Fuc α 1-2Gal β 1-4(Fuc α 1-3)GlcNAc β 1-PAA |
| 15 | α Neu5Ac | PAA | Neu5Gca α 2-PAA |
| 16 | α Neu5Gc | PAA | Neu5Gca α 2-PAA |
| 17 | Sia2 | PAA | Neu5Gca α 2-8Neu5Gca α 2-PAA |
| 18 | Sia3 | PAA | Neu5Gca α 2-8Neu5Gca α 2-8Neu5Gca α 2-PAA |
| 19 | 3'SiaLec | PAA | Neu5Gca α 2-3Gal β 1-3GlcNAc β 1-PAA |
| 20 | 3SL | PAA | Neu5Gca α 2-3Gal β 1-4Glc β 1-PAA |
| 21 | 3'SLN | PAA | Neu5Gca α 2-3Gal β 1-4GlcNAc β 1-PAA |
| 22 | sLea | PAA | Neu5Gca α 2-3Gal β 1-3(Fuc α 1-4)GlcNAc β 1-PAA |
| 23 | sLex | PAA | Neu5Gca α 2-3Gal β 1-4(Fuc α 1-3)GlcNAc β 1-PAA |
| 24 | 6SL | PAA | Neu5Gca α 2-6Gal β 1-4Glc β 1-PAA |
| 25 | FET | Glycoprotein | Fetuin (Complex-type N-glycans and O-glycans) |
| 26 | AGP | Glycoprotein | α 1-acid glycoprotein (Complex-type N-glycans) |
| 27 | TF | Glycoprotein | Transferrin (Complex-type N-glycans) |
| 28 | TG | Glycoprotein | Porcine thyroglobulin (Complex and high-mannose-type N-glycans and O-glycans) |
| 29 | β Gal | PAA | Gal β 1-PAA |
| 30 | [3S] β Gal | PAA | (3SO ₃)Gal β 1-PAA |
| 31 | A-di | PAA | GalNAc α 1-3Gal β 1-PAA |
| 32 | Lac | PAA | Gal β 1-4Glc β 1-PAA |
| 33 | Lec | PAA | Gal β 1-3GlcNAc β 1-PAA |
| 34 | [3'S]Lec | PAA | (3SO ₃)Gal β 1-3GlcNAc β 1-PAA |
| 35 | LN | PAA | Gal β 1-4GlcNAc β 1-PAA |
| 36 | [3'S]LN | PAA | (3SO ₃)Gal β 1-4GlcNAc β 1-PAA |
| 37 | [6S]LN | PAA | Gal β 1-4(6SO ₃)GlcNAc β 1-PAA |
| 38 | [6'S]LN | PAA | (6SO ₃)Gal β 1-4GlcNAc β 1-PAA |
| 39 | β GalNAc | PAA | GalNAc β 1-PAA |
| 40 | d β GalNAc β | PAA | GalNAc β 1-3GalNAc β 1-PAA |
| 41 | LDN | PAA | GalNAc β 1-4GlcNAc β 1-PAA |
| 42 | Ga2 | PAA | GalNAc β 1-4Gal β 1-4Glc β 1-PAA |
| 43 | Asialo-FET | Glycoprotein | Asialo fetuin (Desialylated complex-type N- and O-glycans) |
| 44 | Asialo-AGP | Glycoprotein | Asialo α 1-acid glycoprotein (Desialylated complex-type N-glycans) |
| 45 | Asialo-TF | Glycoprotein | Asialo transferrin (Desialylated complex-type N-glycans) |
| 46 | Asialo-TG | Glycoprotein | Asialo porcine thyroglobulin (Desialylated complex-type N-glycans, high-mannose-type N-glycans) |
| 47 | β GlcNAc | PAA | GlcNAc β 1-PAA |
| 48 | [6S] β GlcNAc | PAA | (6SO ₃)GlcNAc β 1-PAA |
| 49 | Agalacto-Fet | Glycoprotein | Agalacto fetuin (Agalactosylated complex-type N- and O-glycans) |
| 50 | Agalacto-AGP | Glycoprotein | Agalacto α 1-acid glycoprotein (Agalactosylated complex-type N- and O-glycans) |
| 51 | Agalacto-TF | Glycoprotein | Agalacto transferrin (Agalactosylated complex-type N-glycans, high-mannose-type N-glycans) |
| 52 | OVM | Glycoprotein | Ovomucoid (Complex-type N-glycans) |
| 53 | OVA | Glycoprotein | Ovaalbumin (Hybrid-type N-glycans) |
| 54 | α Man | PAA | Man α 1-PAA |
| 55 | β Man | PAA | Man β 1-PAA |
| 56 | [6P]Man | PAA | (6PO ₄)Man α 1-PAA |
| 57 | INV | Glycoprotein | Yeast invertase (High mannose-type N-glycans) |
| 58 | Tn | PAA | GalNAc α 1-PAA |
| 59 | Core1 | PAA | Gal β 1-3GalNAc α 1-PAA |
| 60 | Core2 | PAA | Gal β 1-3(GlcNAc β 1-6)GalNAc α 1-PAA |
| 61 | Core3 | PAA | GlcNAc β 1-3GalNAc α 1-PAA |
| 62 | Core4 | PAA | GlcNAc β 1-3(GlcNAc β 1-6)GalNAc α 1-PAA |
| 63 | Forssman disaccharide | PAA | GalNAc α 1-3GalNAc β 1-PAA |
| 64 | Core6 | PAA | GlcNAc β 1-6GalNAc α 1-PAA |
| 65 | Core8 | PAA | Gal α 1-3GalNAc α 1-PAA |
| 66 | [3'S]Core1 | PAA | (3SO ₃)Gal β 1-3GalNAc α 1-PAA |
| 67 | Gal β -Core3 | PAA | Gal β 1-4GlcNAc β 1-3GalNAc α 1-PAA |
| 68 | Asialo-BSM | Glycoprotein | Asialo bovine submaxillary mucin (Tn) |
| 69 | Asialo-GP | Glycoprotein | Asialo human glycoporphin MN (T) |
| 70 | STn | PAA | Neu5Gca α 2-6GalNAc α 1-PAA |
| 71 | STn (Gc) | PAA | Neu5Gca α 2-6GalNAc α 1-PAA |
| 72 | ST | PAA | Neu5Gca α 2-3Gal β 1-3GalNAc α 1-PAA |
| 73 | Sia2-6Core 1 | PAA | Gal β 1-3(Neu5Gca α 2-6)GalNAc α 1-PAA |
| 74 | BSM | Glycoprotein | Bovine submaxillary mucin (Sialyl Tn) |
| 75 | GP | Glycoprotein | Human glycoporphin (Desialyl T and sialyl Tn) |
| 76 | α Gal | PAA | Gal α 1-PAA |
| 77 | Gal α 1-2Gal | PAA | Gal α 1-2Gal β 1-PAA |
| 78 | Gal α 1-3Gal | PAA | Gal α 1-3Gal β 1-PAA |
| 79 | Gal α 1-3Lac | PAA | Gal α 1-3Gal β 1-4Glc β 1-PAA |
| 80 | Gal α 1-3LN | PAA | Gal α 1-3Gal β 1-4GlcNAc β 1-PAA |
| 81 | Gal α 1-4LN | PAA | Gal α 1-4Gal β 1-4GlcNAc β 1-PAA |
| 82 | Melibiose | PAA | Gal α 1-6Glc β 1-PAA |
| 83 | α Glc | PAA | Glc α 1-PAA |
| 84 | β Glc | PAA | Glc β 1-PAA |
| 85 | Maltose | PAA | Glc α 1-4Glc β 1-PAA |
| 86 | - | - | - |
| 87 | CSA | BSA | Chondroitin Sulfate A-BSA |
| 88 | CSB | BSA | Chondroitin Sulfate B-BSA |
| 89 | HS | BSA | Heparan Sulfate-BSA |
| 90 | HP | BSA | Heparin-BSA |
| 91 | KS | BSA | Keratan Sulfate-BSA |
| 92 | α Rha | PAA | Rhamnosyl-I-PA |
| 93 | Mannan (SC) | Glycoprotein | S. cerevisiae mannan |
| 94 | Mannan (CA) | Glycoprotein | C. albicans mannan |
| 95 | Zymosan | Glycoprotein | Zymosan |
| 96 | Chitobiophage | PAA | GlcNAc β 1-4GlcNAc β 1-PAA |
| 97 | BSA | BSA | - |
| 98 | Negative PAA | PAA | - |
| 99 | Marker | | |
| 100 | BG | | |

Table S2. Oligonucleotide primer sequences used in this study.
Red letters correspond to the codon for an amino acid substitution.

| Primer name | Sequence (5'→3') |
|----------------------|--------------------------------------|
| T7 terminator primer | GCTAGTTATTGCTCAGCGG |
| WA20_H86K_Fw | GACACCGTGCATCATTCAAGAACAAATTGCAGGAGC |
| WA20_caCatg_Fw | gaaggagatatacacATGTATGGCAAGTTGAACAAG |
| H_ACG_Nterm_Fw | catATGACCCTTCAGCCGTGAACATCTAC |
| ACG_Nterm-3_Fw | TCAGCCGTGAACATCTAACACATTAGC |
| WA20_Cterm_Rv | GCGATGTACAAGGTGGTGGAAAG |